ACI STRUCTURAL JOURNAL TECHNICAL PAPER

Title No. 114-S40

Axial Compressive Behavior of CFRP-Confined Expansive Concrete Columns

by Qi Cao, Jinju Tao, Zhongguo John Ma, and Zhimin Wu

Fiber-reinforced polymer (FRP) confined concrete columns use both compressive strength of concrete and tensile strength of FRP efficiently. In this paper, the combination of FRP and expansive concrete was adopted. Ten FRP reinforced concrete disk-shape specimens were made to study the influencing factors of prestress. Eighteen FRP reinforced concrete columns were constructed to investigate the axial compressive behavior. Test variables include the volume ratio of the carbon fiber-reinforced polymer (CFRP) and expansion rate (expansive/non-expansive) of concrete. Based on the results of this investigation, prestress of FRP is found to be inversely proportional to the volume ratio of reinforcement of FRP. The experimental results obtained from the compression tests in terms of stress-strain curves show that the expansive concrete specimens achieved significantly higher inflection stress and ultimate load capacities than conventional non-expansive concrete specimens. Finally, with the effect of prestress taken into account, an improved model aimed at the calculation of the stress at inflection point and ultimate load capacities was proposed. It shows good agreements with experimental results.

Keywords: carbon fiber-reinforced polymer (CFRP); expansive concrete; inflection point; prestress; ultimate load.

INTRODUCTION

With the advantages of lightweight, high strength, good corrosion resistance, and accelerated construction, fiber-reinforced polymer (FRP) confined concrete columns meet the needs of engineering structures, including withstanding heavy load and harsh conditions. In recent years, researchers have conducted extensive work on FRP-confined concrete columns. Many studies have shown that external confinement by wrapping FRP is an efficient technique to increase the load capacity and ductility of the concrete columns.[1-6] The FRP-confined concrete structural system makes full use of tensile properties of FRP and compressive strength of concrete.

It is reported[7] that concrete is a constraint-sensitive material and the lateral expansive deformation of concrete columns under axial compression leads to the tensioning of FRP in radial direction. This causes the core concrete subjected to compressive stress in three directions. Research has shown that the damage of internal concrete occurred when 40 to 50% of the tensile strength of glass fiber-reinforced polymer (GFRP) was reached.[8] It can be inferred that, however, high tensile strength of FRP can only be used after cracking of concrete. This undoubtedly limits the benefits of using FRP materials.

Currently, researchers are focusing on the application of the active confinement on the core concrete by mechanical means of tensioning FRP.[9-11] Test results showed that, due to the effect of prestress, the initial cracking loads are improved and the axial stress at inflection point is increased by 24% compared with the non-prestressed concrete column. However, this method requires specialized equipment and skills, making practical application difficult.

Another solution is filling an FRP tube with expansive concrete. It is aimed to implement active restraint on concrete and generate prestressing force through the expansion of concrete and confinement of FRP. By tensioning FRP through the expansion of concrete, the stress hysteresis of FRP is avoided and internal tension failure of concrete is delayed.

Expansive concrete has been studied in applications of various structural elements. A novel composite structural system using FRP and expansive concrete were developed by Cao et al.[12-14] This hybrid structural system relies on the expansion of concrete and confinement of FRP to generate the prestress. Experimental results show that this system has good potential to eliminate cracking and improve the ultimate load capacity. Another study showed that self-stressing and self-consolidating concrete is very suitable for pouring in steel tube, owing to the curing conditions in the steel tube, which can fully guarantee the occurrence of expansion.[15] To strengthen existing concrete columns, expansive grout was also filled in between the FRP tube and existing concrete columns to achieve prestress.[8] Results showed that the load-bearing capacity of the pretensioned column increased by 35% when compared with non-pretensioned specimens and by 300% compared with unconfined concrete columns. Part of GFRP tube was filled with expansive concrete in the study of El Chabib et al.[16] It was found that expansive concrete created a somewhat better interfacial contact between the two materials. However, study of prestress such as the magnitude and the influencing parameters has not been performed in their research.

RESEARCH SIGNIFICANCE

To date, research on structural performances of highly expansive concrete-filled FRP tube are quite limited. Furthermore, study of influencing parameters on the prestress of the FRP expansive concrete column system has not been

ACI Structural Journal, V. 114, No. 2, March-April 2017.

MS No. S-2016-061.R1, doi: 10.14359/51689450, received June 21, 2016, and reviewed under Institute publication policies. Copyright © 2017, American Concrete Institute. All rights reserved, including the making of copies unless permission is obtained from the copyright proprietors. Pertinent discussion including author's closure, if any, will be published ten months from this journal's date if the discussion is received within four months of the paper's print publication.

Table 1—Mixture proportions and compressive strength

Dosage of expansive agent, %	Cement, kg/m^3	Expansive agent, kg/m^3	Fine aggregate, kg/m^3	Coarse aggregate, kg/m^3	Water, kg/m^3	Compressive strength f_{co}', MPa
0	450	0	636.5	995.5	220	36.76
8	450	36	600.5	995.5	220	35.14
10	450	45	591.5	995.5	220	29.70
12	450	54	582.5	995.5	220	25.14

Notes: 1 kg/m^3 = 0.0624 lb/ft^3; 1 MPa = 145.14 psi.

Fig. 1—Experimental setup of free expansion.

reported. This study provides the experimental data on the parameters study on self-prestress formed in a FRP-confined expansive concrete columns system. Also, presented in this study are the advantages of combining FRP and expansive concrete materials. The data generated from this research will contribute to the understanding of the mechanical properties of FRP-reinforced expansive concrete column, which could be used for real structural application.

EXPERIMENTAL PROGRAM

Concrete mixture design

Currently, lime-system and ettringite-system expansive agents are two commonly used expansive agents. Previous research[12] has shown that the expansion of lime-system concrete is larger than ettringite-system concrete. Test results also indicated that expansion increases with the increase of expansive agent dosage, but the strength of concrete decreased with increasing dosage.[12] Therefore, to obtain a large amount of expansion and proper concrete

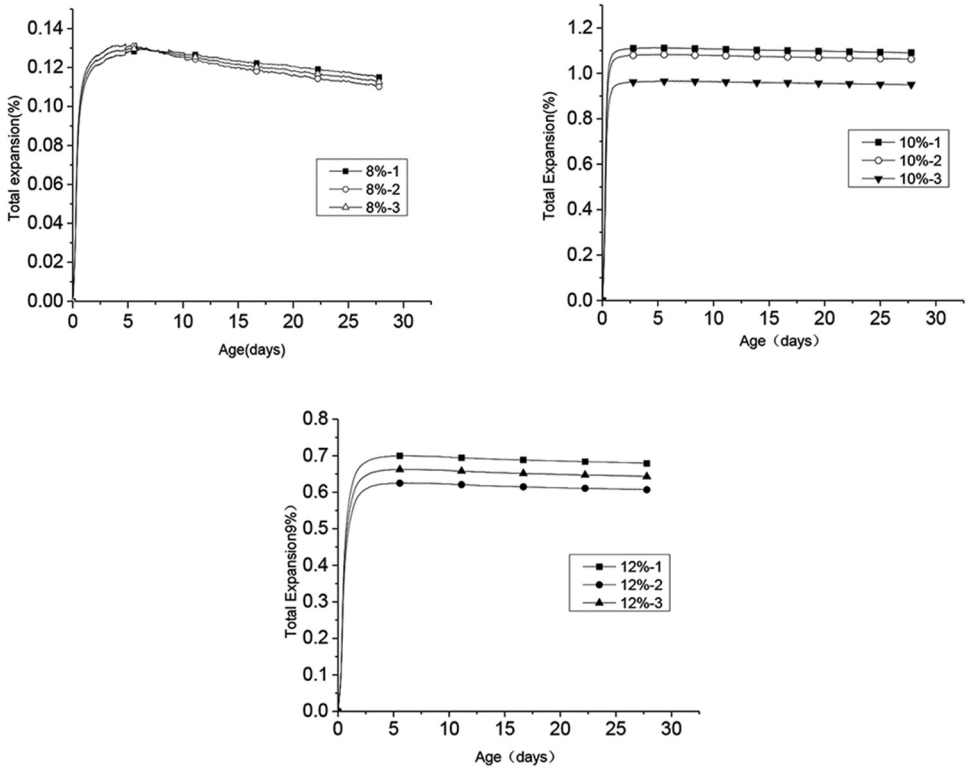

Fig. 2—Experimental results of free expansion.

strength, lime-system expansive agent was used at a certain percentage of cement and it was added to substitute part of sand instead of cement. The mixture proportions of expansive concrete and 28-day compressive strength are shown in Table 1.

Free expansion test

In this experiment, prism specimen with the size of 100 x 100 x 400 mm (3.94 x 3.94 x 15.75 in.) was used to measure the free expansion of concrete. Due to the use of lime-system expansive agent, the expansion of concrete occurred at the early stage. To minimize the effect of casting molds on the expansion of concrete and improve the accuracy of data acquisition, an automatic instrument was used to monitor the expansion of concrete, as shown in Fig. 1. The mold of the instrument was specially designed and could be removed 6 hours after casting of concrete. After that, the expansion of concrete was monitored. The experimental results are shown in Fig. 2.

From Fig. 2, the amount of free expansion of expansive concrete with 10% expansion agent reached 1.02% at 28 days, which is the highest in the three mixtures. It also shows that 10% expansive concrete has achieved a compressive strength of 29.70 MPa (4.31 ksi) at 28 days. The following

Table 2—Material properties of FRP

Thickness, mm/layer	Ultimate strain, microstrain	Elasticity modulus, GPa
0.167	15235	223.70

Notes: 1 mm = 0.0394 in.; 1 GPa = 145.14 ksi.

Table 3—Test matrix of FRP reinforced disc specimens

Specimen		Parameters		
Series	Number	External diameter, mm	Inner diameter, mm	Axial stress, kPa
I	D400-1	400	0	3.6
	D400-2	400	109	3.6
	D400-3	400	220	3.6
	D400-4	400	298	3.6
II	D317-1	317	0	3.6
	D317-2	317	0	7.2
	D317-3	317	0	10.8
III	D200	200	0	3.6
IV	D162	162	0	3.6
V	D110	110	0	3.6

Notes: 1 mm = 0.0394 in.; 1 kPa = 0.145 psi.

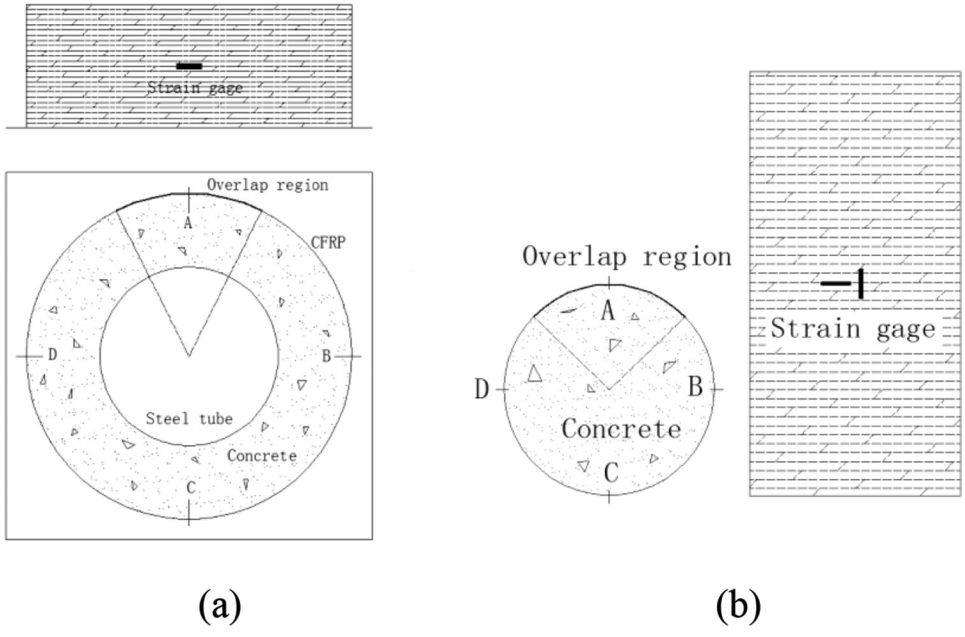

Fig. 3—Layout of strain gauge for: (a) disc specimen; and (b) column specimen.

Fig. 4—Experimental setup for disc-shape specimens.

tests were carried out with the concrete mixture of addition of 10% expansive agent.

FRP property test

Because of high axial tensile strength, high elastic modulus, small thermal expansion, and good corrosion resistance, carbon fiber-reinforced polymer (CFRP) was used as confinement and reinforcement of concrete in this study. The elastic modulus and ultimate tensile strength of CFRP were tested according to ASTM D3039. The properties of CFRP material are listed in Table 2.

Strain monitoring on FRP reinforced expansive concrete disk specimens

A parameters study was conducted using CFRP-reinforced expansive concrete disk specimens. A total of 10 specimens were fabricated with height of 150 mm (5.91 in.). Specimens were designed with different diameters, inner diameters, and axial compression forces. Specimens were divided into five series by the outer diameter, as shown in Table 3. For the labeling of specimens, the first letter "D" represents the Disk specimens, and then a three-digit number represents the outer diameter of the CFRP tube. For Series I, the second number means the inner diameter of steel tube where "1 to 4" represents 0, 109, 220, and 298 mm (0, 4.29, 8.66, and 11.73 in.), respectively. For Series II, the second number represents three different axial stress σ_N where "1 to 3" represents 3.6, 7.2, and 10.8 kPa (0.52, 1.04, and 1.57 psi), respectively.

The external FRP tube was made of CFRP. Precut carbon fiber sheet was wrapped around the mold and the resin adhesive was brushed on the fiber sheet layer-by-layer. The mold was released after 24 hours and CFRP tubes were cured for 7 days at room temperature. All FRP tubes were made of three layers of CFRP laminate. In addition, each FRP tube has an overlap zone with a length of 150 mm (5.91 in.). To monitor the strain of FRP tube, four strain gauges were arranged on the periphery of the FRP at midheight. The arrangement of strain gauge is shown in Fig. 3(a). "ABCD" represents the

Table 4—Test matrix of FRP-reinforced columns

Specimen	Layers of FRP	Dosage of expansive agent, %
C1-0 (3)	1	0
C1-10 (3)	1	10
C3-0 (3)	3	0
C3-10 (3)	3	10
C5-0 (3)	5	0
C5-10 (3)	5	10

Note: Number in parenthese means number of replicated specimens.

(a) (b)

Fig. 5—Axial compression test: (a) experimental setup; and (b) failure mode.

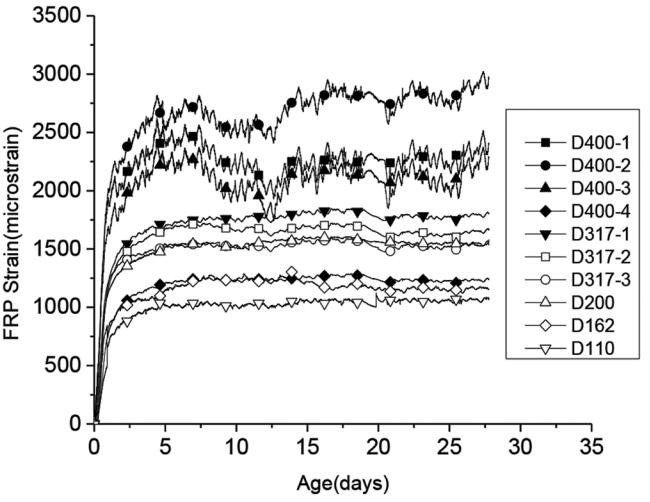

Fig. 6—Strain-time curves of disc specimens.

location of the four strain gauges. For Specimen D400-2 to D400-4, steel tubes with the thickness of 4 mm (0.16 in.) was used as the inside support.

After CFRP tubes were constructed, they were glued on the bottom support. Expansive concrete was poured into the CFRP tube directly. A plastic plate was used to cover the concrete. Several metal weights were stacked on the plastic plate to apply the corresponding axial compression force. The data acquisition system was then connected to monitor the strain of FRP during the curing period until 28 days. The test setup is shown in Fig. 4.

Table 5—Prestress at 28 days of FRP-reinforced disc specimens

Specimen	Strain of FRP ε_{f0}, microstrain	Stress of FRP σ_{f0}, MPa	Stress of concrete σ_{l0}, MPa
D400-1	2397	536	1.34
D400-2	2962	663	1.66
D400-3	2277	509	1.27
D400-4	1245	279	0.70
D317-1	1809	405	1.28
D317-2	1678	375	1.18
D317-3	1582	354	1.12
D200	1537	344	1.72
D162	1153	258	1.59
D110	1087	243	2.21

Note: 1 MPa = 145.14 psi.

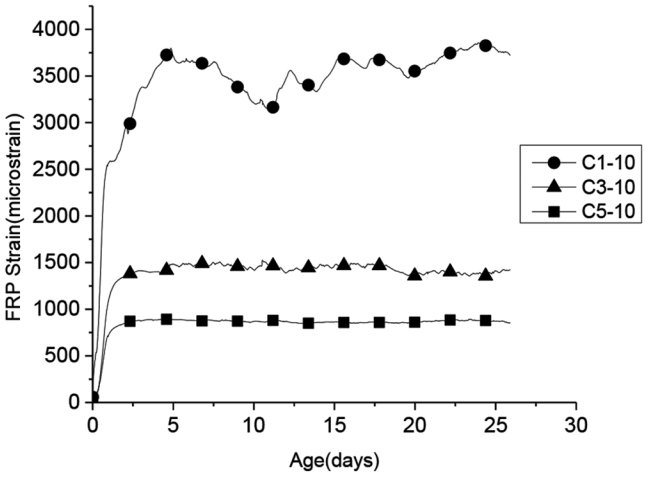

Fig. 7—Strain-time curves of FRP-confined concrete columns.

Table 6—Prestress of FRP-reinforced column at 28 days

Specimen	Experimental strain of FRP, microstrain	Experimental prestress of FRP, MPa	Experimental prestress of concrete, MPa	Calculated prestress of concrete, MPa	Relative error, %	Calculated strain of FRP, microstrain
C1-10	3722	833	1.85	1.546	16.43	3105
C3-10	1422	318	2.12	1.909	9.95	1277
C5-10	855	191	2.13	2.105	1.17	845

Note: 1 MPa = 145.14 psi.

Axial compression test on FRP-reinforced expansive concrete columns

A total of 18 column specimens with 300 mm (11.81 in.) high and 150 mm (5.91 in.) in diameter were made. The variables of the test are composed of FRP reinforcement ratio and the dosage of expansive agent. The experimental matrix is shown in Table 4. The first letter "C" represents the column. The first number that followed letter "C" represents the number of FRP layers, and the second number after "-" represents the dosage of expansive agent in percentage.

The fabrication method of FRP tube was the same as that of previous disk specimens. The length of overlap zone was taken as 150 mm (5.91 in.). To monitor the circumferential and longitudinal strain of the FRP tube, four sets of strain gauges were arranged on the periphery of the FRP tube at midheight. The arrangement of strain gauge is shown in Fig. 3(b), ABCD represents the location of the strain gauges.

After the CFRP tubes were made, they were glued on the support. Concrete was poured in the CFRP tube directly. The plastic sheet was then used to cover the top of the concrete. The data acquisition system was connected to monitor the strain of FRP during the curing period.

An axial compression test was carried out after 28 days from casting of the concrete. The experimental setup is shown in Fig. 5(a). The experiment was conducted on a test machine. The loading is controlled by displacement and the displacement speed is 0.2 mm/min (0.0079 in./min). The load data was collected by a load sensor installed at the base of the specimens and the strain of FRP was collected by the strain gauges installed on the surface of the CFRP.

EXPERIMENTAL RESULTS AND DISCUSSIONS

Result on FRP-reinforced expansive concrete disk specimens

The expansion time curve of the specimen is shown in Fig. 6. The vertical axis in Fig. 6 shows the mean value from four strain gauges. In general, concrete expands intensely during the first 24 hours after being poured and then it tends to expand at a stable rate.

The prestress of concrete and FRP on the 28th day after pouring are shown in Table 5. The prestress in FRP (σ_{f0}) obtained from the 10 specimens is in the range of 243 to 663 MPa (35.27 to 96.23 ksi), and the prestress in concrete (σ_{l0}) is between 0.7 and 2.21 MPa (101.60 and 320.75 psi). Compared with the standards defined by Polivka[17] where prestress for self-stressing concrete is between 1.03 and 3.45 MPa (149.49 and 500.73 psi), it is a relatively high prestress.

Results on FRP-reinforced expansive concrete columns

The prestress-versus-time curves of FRP-confined expansive concrete columns are shown in Fig. 7. The figure shows the similar trend as previous disk specimens that concrete expands intensely during the first 24 hours and then it tends to expand at a stable rate. The prestress of FRP and concrete on the 28th day after pouring are shown in Table 6.

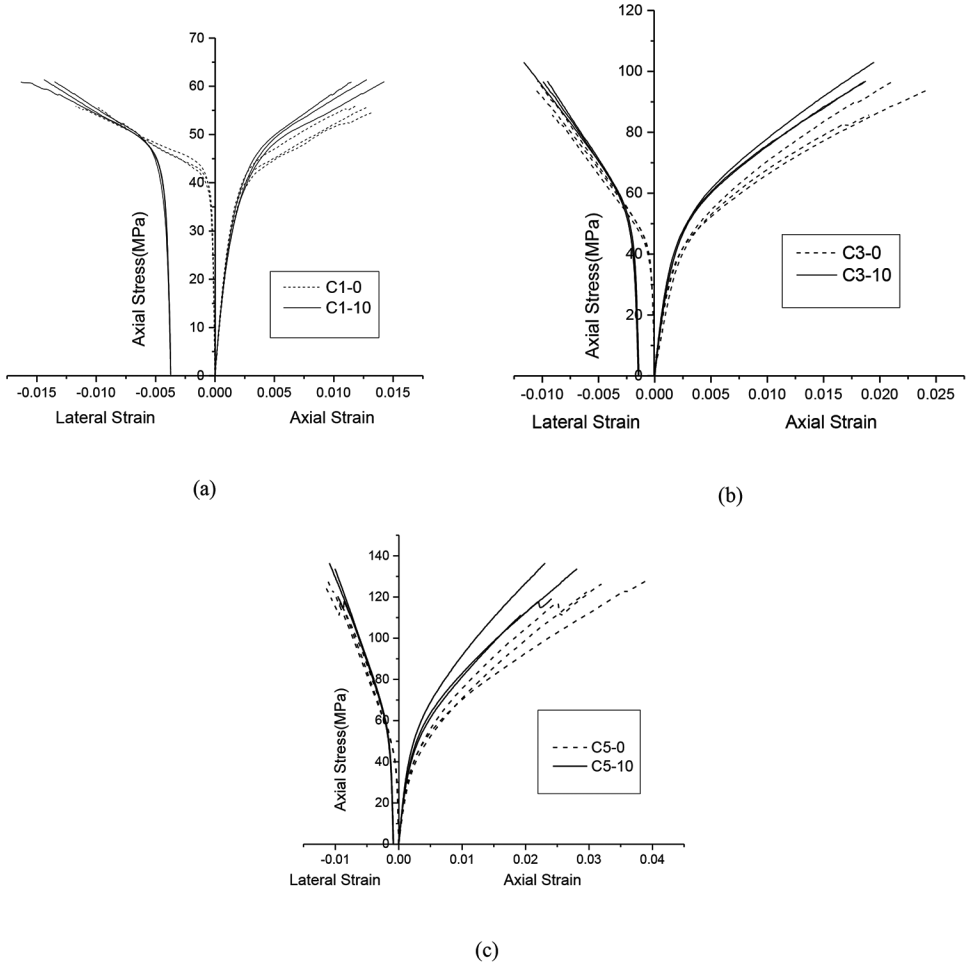

Fig. 8—Stress-strain curves for column specimens: (a) C1 group specimens; (b) C3 group specimens; and (c) C5 group specimens. (Note:1 MPa = 145.14 psi.)

During the axial compression test, the following phenomena were observed. For test specimens without expansive agent, during the initial loading phase, hoop strain increased slowly when the confinement provided by FRP had not yet been exerted and load was sustained mainly by concrete. When the load was close to the ultimate bearing capacity of concrete, due to the lateral deformation of concrete, the circumferential strain of FRP increased rapidly and the role of FRP for lateral confinement was gradually shown. When the load exceeded the limit load of concrete, the increase of the FRP circumferential strain started to stabilize. During that time, the load was sustained mainly by FRP. When the ultimate load was reached, the specimen failed due to the sudden rupture of FRP. For specimens with expansive agent, the failure process was similar to the test specimen without expansive agent. It is worthwhile to notice that, when the role of the FRP for lateral confinement started to show, the axial stress of FRP-confined expansive concrete specimen was much larger than the ultimate bearing capacity of the unconstrained expansive concrete. The typical failure mode of the specimen is shown in Fig. 5(b).

The stress-strain curves of the specimens are shown in Fig. 8. Curves can be divided into three stages: initial linear segment, nonlinear segment, and linear enhancement segment. In the initial linear segment, the load was sustained mainly by the concrete. When the load was close to the ultimate bearing capacity of concrete, due to the development of microcracks in the concrete, the lateral confinement of FRP was activated; the stress-strain curves came into the nonlinear phase. After entering the linear enhancement phase, the stress-strain curve turns into a straight line again. However, the slope is greatly reduced—that is, the axial deformation is greatly increased and the load was sustained mainly by FRP under the fixed load. For FRP-confined expansive concrete specimens, the lateral strain of the stress-strain curve presents an initial value due to the effect of initial prestress.

The diagram in Fig. 9 is used to facilitate the analysis of the prestressing force where the circumferential (hoop) stress is taken as the x-axis coordinate and the axial stress is taken as the y-axis. The intercept of linear enhancement segment is defined as f_o, and the intersection of the initial linear segment and linear enhancement segment is defined as inflection point f_i. Because of the initial prestress, the value of inflection point f_i increased as shown in Fig. 9(b). The mean values of the intercept f_o, inflection point f_i, and ultimate load f_{cu} of each group are shown in Table 7.

In this test, the difference of the mixture proportions between expansive concrete and conventional concrete is that the sand is replaced by the same amount of expansive agent. Therefore, the effect of expansive agent can be

Table 7—Stress at intercept, inflection and ultimate point

Specimen	f_o, MPa	f_o/f_{co}'	Calculated f_o, MPa	Relative error, %	f_i, MPa	f_i/f_o	Calculated f_i, MPa	Relative error, %	f_{cu}, MPa	Calculated f_{cu}, MPa	Relative error, %
C1-0	39.93	1.09	40.07	0.35	39.93	1.00	40.42	1.23	55.17	56.79	2.94
C1-10	40.88	1.38	41.93	2.57	45.40	1.11	47.38	4.36	61.12	60.84	0.46
C3-0	42.08	1.14	40.07	4.78	42.09	1.00	41.10	2.35	92.37	90.24	2.31
C3-10	44.57	1.50	45.24	1.50	52.14	1.17	52.76	1.19	98.69	89.41	9.40
C5-0	41.57	1.13	40.07	3.61	41.59	1.00	41.77	0.43	125.72	123.69	1.61
C5-10	46.32	1.56	46.02	0.65	53.77	1.16	55.07	2.42	129.79	120.67	7.03

Note: 1 MPa = 145.14 psi.

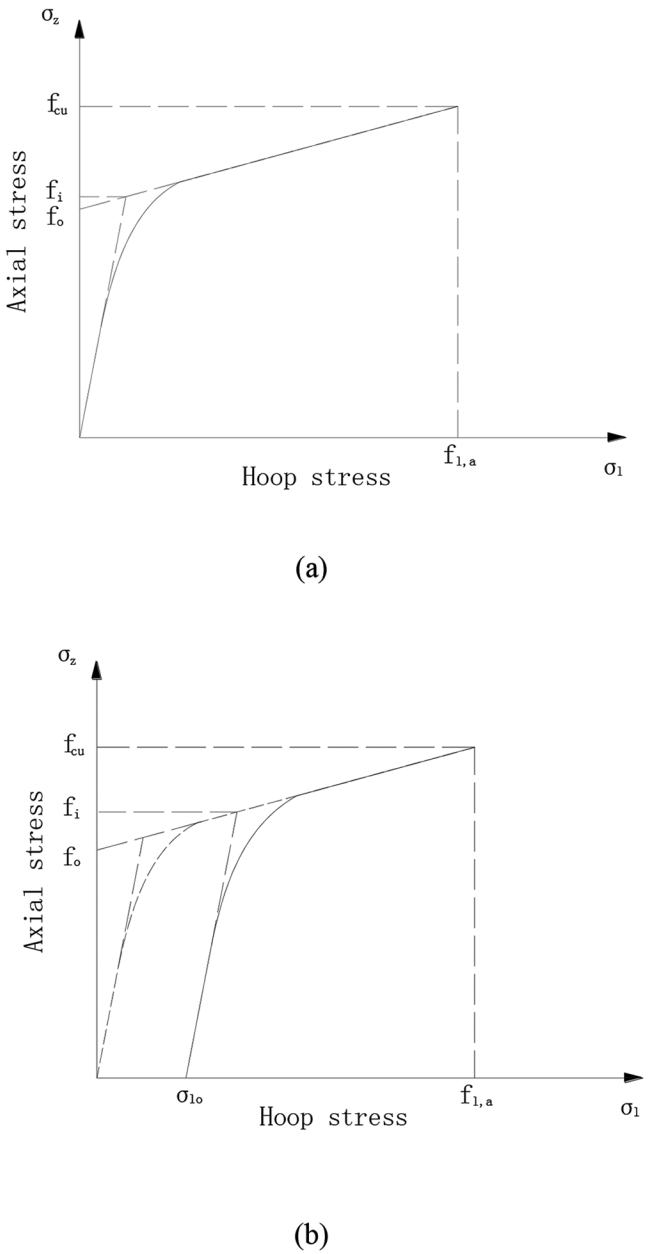

Fig. 9—Schematic diagram of inflection point: (a) nonprestressed specimen; and (b) prestressed specimen.

Table 8—Comparison between expansive concrete specimens and conventional concrete specimens

Specimen	$f_o^e - f_o^{n*}$ (MPa) / percentage†, %	$f_i^e - f_o^e$ (MPa)/ percentage, %	$f_i^e - f_o^n$ (MPa)/ percentage, %	$f_{cu}^e - f_{cu}^n$ (MPa)/ percentage, %
C1-10	0.95/2.38	4.52/11.02	5.47/13.70	5.95/10.78
C3-10	2.49/5.92	7.57/16.98	10.06/23.88	6.32/6.84
C5-10	4.75/11.42	7.45/16.08	12.2/29.29	4.07/3.24

*Superscripts e and n are used to denote expansive concrete and non-expansive concrete.

†Percentage is $(f_o^e - f_o^n)/f_o^n$.

Note: 1 MPa = 145.14 psi.

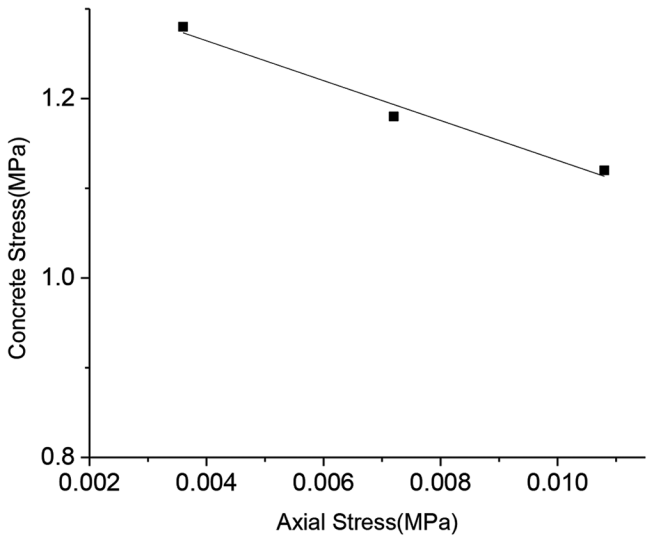

Fig. 10—Relationship between prestress and applied axial force. (Note:1 MPa = 145.14 psi.)

obtained by comparing the two groups of specimens. The comparison results are shown in Table 8. The effect of expansion agent in FRP-restrained expansive concrete column can be mainly divided into two parts. First, due to the expansion of concrete under the constraints of FRP, the product of the expansion reaction tends to fill the inner holes and interfacial transition zone (ITZ), making the interior structure of concrete denser. This causes the compressive strength of expansive concrete higher than that of concrete without

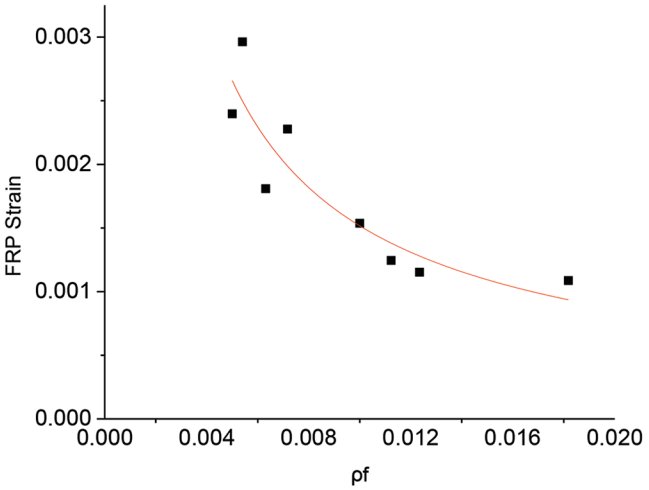

Fig. 11—Relationship between initial strain of FRP and volume ratio of reinforcement.

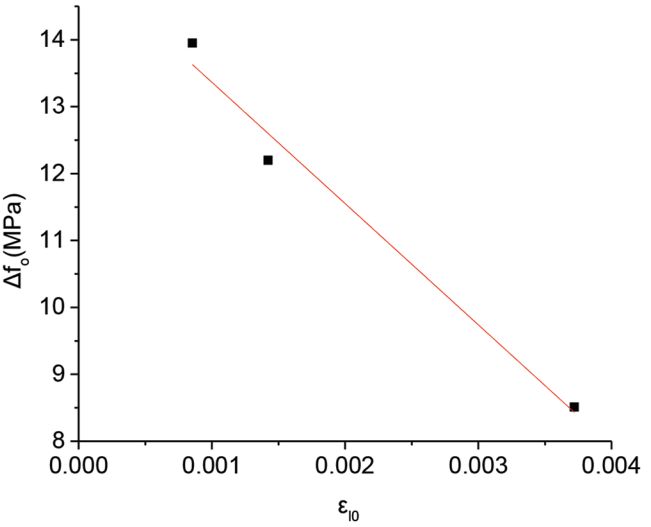

Fig. 12—Relationship between Δf_o and initial strain of concrete ε_{l0}. (Note: 1 MPa = 145.14 psi.)

expansive agent, which is much larger than the strength of unconfined expansive concrete. Previous research[18] has shown that the average ratio of f_o/f_{co}' is 1.09 with a standard deviation of 0.13. According to Table 8, due to the confinement of FRP the f_o of the expansive concrete is increased by 0.95 to 4.75 MPa (137.88 to 689.40 psi). The increment of strength increases with the increase of the reinforcement ratio of FRP, and the ratio of highest increment is 11.42%. Next, due to the expansion of concrete, FRP is tensioned and prestress is formed in FRP and concrete. The stress at inflection point is then improved. As shown in Table 7, for conventional concrete specimens, f_i^n and f_o^n (the superscripts n is used to represent non-expansive concrete) are very close. However, it shows clearly that for expansive concrete specimens, the difference between f_i^e and f_o^e (the superscripts e is used to represent expansive concrete), that is, ($f_i^e - f_o^e$) becomes larger, which is mainly caused by the effect of prestress. As shown in Table 8, the stress value of the inflection point of the specimen is increased by 4.52 to 7.45 MPa (656.02 to 1081.28 psi), and the ratio of highest increment is 17%. When the two parts are taken into account together, the inflection point of the tested specimen is increased by 5.47 to 12.2 MPa (793.90 to 1770.68 psi). The ratio of highest increment is 29.29%, which has exceeded the increment shown by Zīle et al.[10] by means of tensioning FRP. It can be seen clearly from Table 8 that the ultimate load capacity of concrete column has also been improved.

THEORETICAL CALCULATIONS AND DISCUSSION

Relationship between prestress in concrete σ_{l0} and axial stress σ_N in disk specimens

Figure 10 shows the relationship between prestress in concrete σ_{l0} and axial stress σ_N of series II disk specimens. It shows that the prestress in concrete σ_{l0} decreases with the increase of the axial stress σ_N. It shows a linear relationship and the regression equation is shown as follows

$$\sigma_{l0} = 1.35 - 22.22 \times \sigma_N \quad (1)$$

In this experiment, the active confinement was applied by putting metal weights on the top of the specimens. This method shows a negative effect on the expansion of concrete, which reduces the prestress in concrete. Therefore, it can be speculated that if no axial constraint or a passive axial constraint was applied, higher prestress could be expected.

Relationship between prestress in concrete σ_{l0} and volume ratio of reinforcement ρ_f in disk specimens

The strain of FRP is related to the volume of expansive concrete.[8] At the same time, it is related to the stiffness of FRP.[12] Combining the previous two factors, the volume ratio of reinforcement ρ_f as shown in Eq. (2) is used as the major influencing factor for prestress in concrete σ_{l0}.

$$\rho_f = 2\pi RtH / \pi\left(R^2 - r^2\right)H \quad (2)$$

where t is the thickness of FRP; R is the radius of the specimens; r is the inner diameter of the disk specimen; and H is the height of the specimens.

Figure 11 shows the relationship between FRP strain of all disk specimens with equal axial stress and volume ratio of reinforcement. The results demonstrate that initial strain of FRP ε_{f0} decreases with the increase of the volume ratio of reinforcement. Due to the condition of strain compatibility, $\varepsilon_{f0} = \varepsilon_{l0}$. The following regression equation relating ε_{l0} to ρ_f is obtained

$$\varepsilon_{l0} = \varepsilon_{f0} = 3.67 \times 10^{-5} \rho_f^{-0.808} \quad (3)$$

Equations (4) and (5) show prestress in FRP and concrete, respectively

$$\sigma_{f0} = E_f \varepsilon_{f0} \quad (4)$$

where, E_f is the elastic modulus of FRP.

$$\sigma_{l0} = E_f \varepsilon_{f0} t / R \quad (5)$$

As pointed out in earlier discussion and Eq. (1), prestress σ_{l0} is linearly correlated with axial stress σ_N. Considering the effect of σ_N, a correlation coefficient α was incorporated in Eq. (3).

$$\varepsilon_{l0} = \varepsilon_{f0} = 3.67 \times 10^{-5} \alpha \rho_f^{-0.808} \quad (6)$$

Equation (3) was obtained based on the condition of σ_N = 0.0036 MPa (0.52 psi). To keep Eq. (6) the same as Eq. (3), α should be equal to 1 when σ_N = 0.0036 MPa (0.52 psi). Therefore, Eq. (1) is divided by $\sigma_{l0}|\sigma_{N=0.0036}$ and it becomes $\alpha = 1.06 - 17.50\sigma_N$.

Prestress in FRP-reinforced expansive column specimens

The results of the calculated prestress of the FRP column are shown in Table 6 according to Eq. (5). It shows that the calculated stress values are quite close to the experimental result. As indicted in Table 6, the prediction accuracy is higher when the CFRP reinforcement ratio is higher (1.17% for five-layer CFRP versus 16.43% for one-layer CFRP).

Intercept f_o

It can be seen from Table 7 that the average ratio of $f_o^n/f_{co}^{n\prime}$ (superscript *n* is used to represent non-expansive concrete) for specimens without expansive agent is in good agreement with the previous results.[18] But for specimens with expansive agent the average ratio of $f_o^e/f_{co}^{e\prime}$ (superscripts *e* is used to represent expansive concrete) is larger than 1.09. This may be due to the expansion of concrete confined by FRP making the interior structure of concrete denser as explained previously. The relationship between Δf_o and initial strain of concrete ε_{l0} is shown in Fig. 12 where $\Delta f_o = f_o^e - 1.09 f_{co}^{e\prime}$. It shows a good linear relationship, and the regression equation is shown as follows

$$\Delta f_o = 15.18 - 1.81\varepsilon_{l0} \times 10^3 \quad (7)$$

In this paper, intercept f_o was taken as $f_o^n = 1.09 f_{co}^{n\prime}$ for non-expansive concrete. For expansive concrete, according to Eq. (7) and the definition of Δf_o, it was taken as follows

$$f_o^e = 1.09 f_{co}^{e\prime} + \Delta f_o = 1.09 f_{co}^{e\prime} - 1.81\varepsilon_{l0} \times 10^3 + 15.18 \quad (8)$$

The comparison between test and calculation results is shown in Table 7. The experimental and calculated values are in a good agreement (0.35 to 4.78%).

Stress at inflection point f_i

As stated earlier, the stress-strain curves can be divided into three stages. In the initial linear segment, assuming Hooke's law for concrete, the lateral strain ε_l is[10,11]

$$\varepsilon_l = \frac{1}{E_c}\left[\sigma_l - \nu(\sigma_l + \sigma_z)\right] \quad (9)$$

where σ_l and σ_z are the hoop and axial strain of the columns, respectively. In this paper, compression strain and stresses

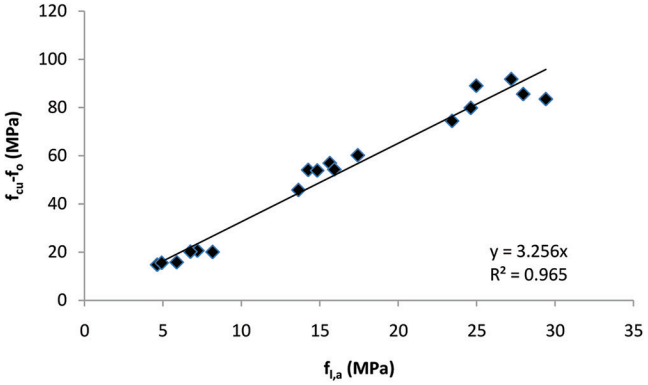

Fig. 13—Relationship between f_{cu}-f_o *and actual maximum limit pressure. (Note: 1 MPa = 145.14 psi.)*

are taken as positive; tension strain and stresses are taken as negative. ν is the Poisson's ratio of concrete and is taken as $\nu = 8 \times 10^{-6} f_{co}'^2 + 0.0002 f_{co}' + 0.138$[19]; E_c is the elastic modulus of concrete, $E_c = 4730\sqrt{f_{co}'}$.[20] For expansive concrete, because the concrete was confined and prestressed by FRP, the compressive strength is much larger than $f_{co}'^e$. Therefore, in calculation of ν and E_c, adjusted compressive strength $f_{co}'^e$ was used instead. Previous research[18] has shown that the average ratio of f_o/f_{co}' is 1.09, therefore $f_{co}'^e = f_o^e/1.09$ was adopted.

Considering condition of strain compatibility $\varepsilon_f = \varepsilon_l$, the relation between ε_l and σ_l is

$$\varepsilon_l = \varepsilon_f = -\frac{R\sigma_l}{tE_f} \quad (10)$$

Combining Eq. (9) and (10), the relationship between σ_l and σ_z is[10,11]

$$\sigma_l = \frac{k\nu}{1 + k(1-\nu)}\sigma_z \quad (11)$$

where k is a parameter to characterize the stiffness of FRP, $k = \frac{tE_f}{RE_c}$

For the linear enhancement segment, the intercept is f_o. At the end of the linear enhancement segment, the ultimate tensile strain of FRP was reached, namely, σ_l equals to the actual maximum limit pressure $f_{l,a} = \frac{E_f t}{R}\varepsilon_{h,rup}$.

where $\varepsilon_{h,rup}$ is the circumferential fracture strain, $\varepsilon_{h,rup} = k_{\varepsilon,f}\varepsilon_h$, for the specimen with expansive agent, because of the initial prestress, $\varepsilon_{h,rup}$ should subtract the initial expansion strain ε_{f0}; ε_h is the ultimate strain of FRP from flat coupon test; $k_{\varepsilon,f}$ is the circumferential fracture strain reduction factor of FRP, which is taken as $k_{\varepsilon,f} = 0.9 - 2.3 f_{co}' \times 10^{-3} - 0.75E_f \times 10^{-6}$.[21] For the expansive concrete, taking into the role of prestressing, the regression relation obtained is $k_{\varepsilon,f} = 0.9 - 2.3 f_{co}' \times 10^{-3} - 0.75E_f \times 10^{-6} + 0.596\sigma_{f0}^2 \times 10^{-6} - 0.129\sigma_{f0} \times 10^{-3}$ (when $k_{\varepsilon,f} > 1$, take $k_{\varepsilon,f} = 1$).

The variable σ_z is equal to the ultimate load capacity f_{cu} at this point. Set $f_{l,a}$ and f_{cu}-f_o of all specimens as x-axis and y-axis, respectively, as shown in Fig. 13. The slope of the

linear enhancement segment is 3.26, which is obtained from linear fitting in Fig. 13.

For the linear enhancement segment, regression relation obtained

$$\sigma_z = f_o + 3.26 \cdot \sigma_1 \tag{12}$$

Combining Eq. (11) and (12), the stress at inflection point can be expressed as

$$f_i = \frac{1 + k(1-\nu)}{1 + k - 4.26k\nu} f_o \tag{13}$$

However, due to the role of prestress, Eq. (11) turns into

$$\sigma_1 = \frac{k\nu}{1 + k(1-\nu)} \sigma_z + \sigma_{10} \tag{14}$$

where σ_{10} is the value of prestress in concrete, which is calculated by using Eq. (5).

Combining Eq. (12) and (14), the stress at inflection point when considering the prestress is shown as follows

$$f_i = \left(\frac{1 + k(1-\nu)}{1 + k - 4.26k\nu} \right) \left(f_o + 3.26\sigma_{10} \right) \tag{15}$$

The experimental and calculated results using Eq. (13) and (15) for the stress of inflection point are shown in Table 7. From the table, it can be seen that the calculated results are in good agreement with the experimental ones (deviations are between 0.43% and 4.36%).

Ultimate load capacity f_{cu}

It was observed in the test that the final failure of the specimen was caused by FRP rupture. At the end of the linear enhancement segment, ultimate tensile strain of FRP was reached, namely, $\sigma_l = f_{l,a}$. And σ_z equals to the ultimate load capacity f_{cu} at this point. Therefore, Eq. (12) becomes

$$f_{cu} = f_o + 3.26 \cdot f_{l,a} \tag{16}$$

The comparison between test and calculation results is shown in Table 7. The experimental and calculated values are in good agreement with deviations between 0.46% and 9.40%.

CONCLUSIONS

The following conclusions can be drawn based on the experimental investigation and theoretical analysis of FRP-reinforced expansive concrete disk and column specimens:

1. The prestress of FRP is related to the volume ratio of reinforcement of the specimen. Axial active confinement has a negative effect on the expansion of concrete, leading to reduction in prestress in concrete.

2. For FRP-reinforced expansive concrete columns specimens, prestress in concrete caused by expansion of concrete and confinement is in the range of 1.85 to 2.13 MPa (268.51 to 309.14 psi), which is quite significant.

3. Due to the expansion of the concrete, the interior structure of concrete becomes denser, and the axial compressive strength of expansive concrete exceeds that of the concrete without expansive agent, which is much higher than that of unconfined expansive concrete.

4. Due to the expansion of concrete, prestress is generated in FRP and concrete, and the range of the initial linear segment is improved. The stress at inflection point was increased by 17% for three-layer CFRP reinforcement, which is the highest among all.

5. On the basis of the existing calculation models, with the effect of prestress taken into account, calculated results of the stress at inflection point and the ultimate load are in good agreement with the experimental data.

AUTHOR BIOS

Qi Cao *is an Assistant Professor at the State Key Laboratory of Coastal and Offshore Engineering, and Ocean Engineering Joint Research Center of DUT-UWA, Dalian University of Technology, Liaoning, China. He received his MS from Washington State University, Pullman, WA, and his PhD from the University of Tennessee Knoxville, Knoxville, TN, respectively. His research interests include high-performance cementitious materials and fiber-reinforced polymer composites.*

Jinju Tao *is a Masters Candidate at the State Key Laboratory of Coastal and Offshore Engineering, Dalian University of Technology. His research interests include fiber-reinforced polymer-confined concrete structures and expansive concrete application in structures.*

ACI member **Zhongguo John Ma** *is a Professor in the Department of Civil and Environmental Engineering at the University of Tennessee, Knoxville. He is a member of Joint ACI-ASCE Committees 343, Concrete Bridge Design, and 445, Shear and Torsion. His research interests include prestressed concrete, fiber-reinforced polymer composites, and sustainable structures.*

Zhimin Wu *is a Professor at the State Key Laboratory of Coastal and Offshore Engineering, Dalian University of Technology, where he received his BS, MS, and PhD. His research interests include bond behavior of reinforcement, fracture mechanics of concrete, and rehabilitation of existing concrete structures.*

ACKNOWLEDGMENTS

Authors would like to acknowledge the financial support provided by the National Natural Science Foundation of China under the grants of NSFC 51208077, 51421064, and 51478084.

REFERENCES

1. Mirmiran, A., and Shahawy, M., "Behavior of Concrete Columns Confined by Fiber Composites," *Journal of Structural Engineering*, ASCE, V. 123, No. 5, 1997, pp. 583-590. doi: 10.1061/(ASCE)0733-9445(1997)123:5(583)

2. Xiao, Y., and Wu, H., "Compressive Behavior of Concrete Confined by Carbon Fiber Composite Jackets," *Journal of Materials in Civil Engineering*, ASCE, V. 12, No. 2, 2000, pp. 139-146. doi: 10.1061/(ASCE)0899-1561(2000)12:2(139)

3. Valdmanis, V.; De Lorenzis, L.; Rousakis, T.; and Tepfers, R., "Behaviour and Capacity of CFRP-Confined Concrete Cylinders Subjected to Monotonic and Cyclic Axial Compressive Load," *Structural Concrete*, V. 8, No. 4, 2007, pp. 187-200. doi: 10.1680/stco.2007.8.4.187

4. Yu, T.; Fang, X. L.; and Teng, J. G., "FRP-Confined Self-Compacting Concrete under Axial Compression," *Journal of Materials in Civil Engineering*, ASCE, V. 26, No. 11, 2014, pp. 04014082 doi: 10.1061/(ASCE)MT.1943-5533.0000993

5. Campione, G.; La Mendola, L.; Monaco, A.; Valenza, A.; and Fiore, V., "Behavior in Compression of Concrete Cylinders Externally Wrapped with Basalt Fibers," *Composites. Part B, Engineering*, V. 69, 2015, pp. 576-586. doi: 10.1016/j.compositesb.2014.10.008

6. Deng, Z. C., and Qu, J. L., "The Experimental Studies on Behavior of Ultrahigh-Performance Concrete Confined by Hybrid Fiber-Reinforced Polymer Tubes," *Advances in Materials Science and Engineering*, V. 2015, 2015, 18 pp. doi: 10.1155/2015/201289

7. Samaan, M.; Mirmiran, A.; and Shahawy, M., "Model of Concrete Confined by Fiber Composites," *Journal of Structural Engi-*

neering, ASCE, V. 124, No. 9, 1998, pp. 1025-1031. doi: 10.1061/(ASCE)0733-9445(1998)124:9(1025)

8. Mortazavi, A. A.; Pilakoutas, K.; and Son, K. S., "RC Column Strengthening by Lateral Pre-Tensioning of FRP," *Construction and Building Materials*, V. 17, No. 6-7, 2003, pp. 491-497. doi: 10.1016/S0950-0618(03)00046-1

9. Tamuzs, V.; Tepfers, R.; and Sparnins, E., "Behavior of Concrete Cylinders Confined by Carbon-Composite 2. Prediction of Strength," *Mechanics of Composite Materials*, V. 42, No. 2, 2006, pp. 109-118. doi: 10.1007/s11029-006-0022-7

10. Zīle, E.; Daugevicius, M.; and Tamuzs, V., "The Effect of Pretensioned FRP Windings on the Behavior of Concrete Columns in Axial Compression," *Mechanics of Composite Materials*, V. 45, No. 5, 2009, pp. 457-466. doi: 10.1007/s11029-009-9107-4

11. Ciniņa, I.; Zīle, E.; and Zīle, O., "Mechanical Behavior of Concrete Columns Confined by Basalt FRP Winding," *Mechanics of Composite Materials*, V. 48, No. 5, 2012, pp. 539-546. doi: 10.1007/s11029-012-9298-y

12. Cao, Q., and Ma, Z. J., "Behavior of Externally Fiber-Reinforced Polymer Reinforced Shrinkage-Compensating Concrete Beams," *ACI Structural Journal*, V. 108, No. 5, Sept.-Oct. 2011, pp. 592-600.

13. Cao, Q., and Ma, Z. J., "Structural Behavior of FRP Enclosed Shrinkage-Compensating Concrete (SHCC) Beams Made with Different Expansive Agents," *Construction and Building Materials*, V. 75, 2015, pp. 450-457. doi: 10.1016/j.conbuildmat.2014.11.045

14. Cao, Q.; Tao, J.; and Ma, Z. J., "Prestress Loss in Externally FRP Reinforced Self Prestressing Concrete Beams," *Construction and Building Materials*, V. 101, 2015, pp. 667-674. doi: 10.1016/j.conbuildmat.2015.10.147

15. Carballosa, P.; Garcia Calvo, J. L.; Revuelta, D.; Sánchez, J. J.; and Gutiérrez, J. P., "Influence of Cement and Expansive Additive Types in the Performance of Self-Stressing and Self-Compacting Concretes for Structural Elements," *Construction and Building Materials*, V. 93, 2015, pp. 223-229. doi: 10.1016/j.conbuildmat.2015.05.113

16. El Chabib, H.; Nehdi, M.; and El Naggar, M. H., "Behavior of SCC Confined in Short GFRP Tubes," *Cement and Concrete Composites*, V. 27, No. 1, 2005, pp. 55-64. doi: 10.1016/j.cemconcomp.2004.02.045

17. Polivka, M., "Factors Influencing Expansion of Expansive Cement Concretes," *ACI Special Publications*, V. 38, 1973, pp. 239-250.

18. Lam, L., and Teng, J. G., "Design-Oriented Stress-Strain Model for FRP-Confined Concrete," *Construction and Building Materials*, V. 17, No. 6-7, 2003, pp. 471-489. doi: 10.1016/S0950-0618(03)00045-X

19. Candappa, D. C.; Sanjayan, J.; and Setunge, S., "Complete Triaxial Stress-Strain Curves of High-Strength Concrete," *Journal of Materials in Civil Engineering*, ASCE, V. 13, No. 3, 2001, pp. 209-215. doi: 10.1061/(ASCE)0899-1561(2001)13:3(209)

20. ACI, Committee 318, "Building Code Requirements for Structural Concrete (ACI 318-14) and Commentary (ACI 318R-14)," American Concrete Institute, Farmington Hills, MI, 2014, 519 pp.

21. Ozbakkaloglu, T., and Lim, J. C., "Axial Compressive Behavior of FRP-Confined Concrete: Experimental Test Data Base and a New Design-Oriented Model," *Composites. Part B, Engineering*, V. 55, 2013, pp. 607-634. doi: 10.1016/j.compositesb.2013.07.025